Biosensors and Bioelectronics 200 (2022) 113861

Contents lists available at ScienceDirect

Biosensors and Bioelectronics

journal homepage: www.elsevier.com/locate/bios

Reagentless electrochemical biosensors through incorporation of unnatural amino acids on the protein structure

Elnaz Zeynaloo [a,c], Elsayed M. Zahran [b], Yu-Ping Yang [a,d], Emre Dikici [a,d,e], Trajen Head [a,d], Leonidas G. Bachas [c,d], Sylvia Daunert [a,d,e,*]

[a] Department of Biochemistry and Molecular Biology, Miller School of Medicine, University of Miami, Miami, FL, 33136, United States
[b] Department of Chemistry, Ball State University, Muncie, IN, 47306, United States
[c] Department of Chemistry, University of Miami, Miami, FL, 33134, United States
[d] Dr. JT Macdonald Foundation Biomedical Nanotechnology Institute, University of Miami, Miami, FL, 33136, United States
[e] Clinical and Translational Science Institute, University of Miami, Miami, FL, 33136, United States

ARTICLE INFO

Keywords:
Electrochemical biosensor
Unnatural amino acid
L-DOPA
Protein labeling
Glucose sensor

ABSTRACT

Typical protein biosensors employ chemical or genetic labeling of the protein, thus introducing an extraneous molecule to the wild-type parent protein, often changing the overall structure and properties of the protein. While these labeling methods have proven successful in many cases, they also have a series of disadvantages associated with their preparation and function. An alternative route for labeling proteins is the incorporation of unnatural amino acid (UAA) analogues, capable of acting as a label, into the structure of a protein. Such an approach, while changing the local microenvironment, poses less of a burden on the overall structure of the protein. L-DOPA is an analog of phenylalanine and contains a catechol moiety that participates in a quasi-reversible, two-electron redox process, thus making it suitable as an electrochemical label/reporter. The periplasmic glucose/galactose binding protein (GBP) was chosen to demonstrate this detection principle. Upon glucose binding, GBP undergoes a significant conformational change that is manifested as a change in the electrochemistry of L-DOPA. The electroactive GBP was immobilized onto gold nanoparticle-modified, polymerized caffeic acid, screen-printed carbon electrodes (GBP-LDOPA/AuNP/PCA/SPCE) for the purpose of direct measurement of glucose levels and serves as a proof-of-concept of the use of electrochemically-active unnatural amino acids as the label. The resulting reagentless GBP biosensors exhibited a highly selective and sensitive binding affinity for glucose in the micromolar range, laying the foundation for a new biosensing methodology based on global incorporation of an electroactive amino acid into the protein's primary sequence for highly selective electrochemical detection of compounds of interest.

1. Introduction

Bioreceptor molecules, such as proteins, are powerful molecular recognition elements that can be used in the detection of a range of analytes. Labeling such biomolecules with a reporter compound can lead to simplified methods in which binding of the analyte causes a change in the signal produced by the reporter (Joel et al., 2014). Most such methods involve the labeling of proteins with fluorescent molecules and monitoring the change in fluorescence (directly or through FRET) upon analyte binging. Labeling proteins with electrochemical reporters is mostly accomplished through chemical attachment of an electroactive molecule to the amino group of lysines or the thiol group of cysteines. Because of the size of the electroactive molecule the overall structure of the parent protein may change, and its functionality may be altered. Incorporating amino acid analogues that are electroactive at specific locations within the protein structure provides a powerful alternative because it allows for protein folding that is similar to the native protein, increasing the probability that functionality is maintained. Such amino acid incorporation can be performed by using amber codon suppression and tRNA/synthetase pairs to substitute an amino acid with an unnatural one at specific locations (Strømgaard et al., 2004; Smolskaya and Andreev, 2019). This process, however, is more cumbersome than using an auxotrophic strain that is unable to synthesize a particular amino acid (Wang and Schultz, 2002; Kato, 2015). Growing such a strain in the

* Corresponding author. Department of Biochemistry and Molecular Biology, Miller School of Medicine, University of Miami, Miami, FL, 33136, United States.
E-mail address: sdaunert@med.miami.edu (S. Daunert).

https://doi.org/10.1016/j.bios.2021.113861
Received 7 October 2021; Received in revised form 19 November 2021; Accepted 1 December 2021
Available online 7 December 2021
0956-5663/

presence of an unnatural amino acid analogue allows incorporation of the latter in the protein structure. In this work we evaluated a strategy to incorporate directly, and during protein synthesis, electroactive unnatural amino acids (UAAs) into the structure of the protein using an auxotrophic strain and the periplasmic glucose/galactose binding protein (GBP) as a model.

GBP is a member of the sugar-binding protein subclass of PBPs that has been used as a platform for designing binding proteins with novel ligand specificities (Looger et al., 2003). The GBP's glucose-binding site is located within the interface between the two domains of the protein. The location of this glucose-binding site is similar among structurally characterized periplasmic sugar-binding proteins. Sugar binding proceeds from an encounter complex with the open form of the protein, the predominant protein conformation in the absence of ligand, followed by hinge bending to give the closed form (Palani et al., 2012). Hydrogen-bonding and hydrophobic interactions of the sugar with both protein domains stabilize the closed form (Vyas et al., 1988). GBP has been successfully used as a bioreporter molecule by our group and others to develop biosensors (Salins et al., 2001a; Teasley Hamorsky et al., 2008). We have previously shown the design of a reagentless sensing system based on a fluorescently labeled GBP with submicromolar glucose detection limits (Salins et al., 2001b; Ehrick et al., 2009). Additionally, we have developed an optical glucose biosensor based on semisynthetic glucose recognition proteins (GPRs) with enhanced thermal stability and a larger detection range. The GPRs were prepared by truncation of GBP and global incorporation of UAAs (7-azatryptophan and 5-fluorotryptophan) into the structure of GBP and its fragments (Joel et al., 2014). Thus, GBP has proven to be an excellent model protein for the development of protein biosensors based on binding proteins, and, importantly, incorporation of unnatural amino acids into its parent structure. This provides a strong scientific support for our premise that incorporation of electroactive unnatural amino acids into a protein structure should yield a protein that can generate an electrochemical signal, and, further, that this signal can be correlated to a binding event in the protein. To that end, in the present study, we evaluated the feasibility of using different UAAs in the design and development of electrochemical reagentless label-free biosensors using binding proteins.

A great amount of effort has been put into developing electrochemical sensors that are selective and sensitive to the analyte of interest through the use of nanomaterials, addition of different catalysts and mediators, and application of innovative bioreceptors. A number of studies have reported the successful fabrication of biologically relevant sensors containing composite structures of several components such as enzymes (Rernglit et al., 2019), metal nanoparticles (Mathew and Sandhyarani, 2014; Fazio et al., 2021), and conductive polymers (Bagdziunas and Palinauskas, 2020; Teran-Alcocer et al., 2021) to selectively detect the analyte in different types of media with high sensitivity. The incorporation of nanomaterials is a new promising trend in the fabrication of electrochemical biosensors leading to improvements in sensitivity, linear detection range, limit of detection, electrical conductivity, and also providing a more effective bioreceptor immobilization (Zeng et al., 2016).

Gold nanoparticles (AuNPs) have been utilized in the fabrication of electrochemical biosensors, including non-enzymatic glucose biosensors (Heo et al., 2012; Sehit et al., 2020). AuNPs have excellent biocompatibility and facilitate the conjugation of the bioreceptors on the surface of the electrode. Additionally, the large surface-to-volume ratio of AuNPs increases sensor sensitivity. We have previously exploited these properties to fabricate a non-enzymatic glutamate biosensor using glutamate binding protein conjugated to AuNPs on the surface of screen-printed carbon electrodes (SPCE) (Bachas et al., 2019; Mohapatra et al., 2020; Zeynaloo et al., 2021a).

Herein, we evaluated the use of an *E. coli* phenylalanine (Phe) auxotroph to incorporate 3,4-dihydroxyphenylalanine (L-DOPA) or 3-amino-L-tyrosine (NH_2Y) as unnatural electroactive amino acids into the structure of a periplasmic binding protein, namely GBP. The redox-active UAA can act as a reporter molecule to generate an electrochemically active bioreporter. The biosensor was fabricated using a screen-printed carbon electrode (SPCE) decorated with a thin film of polycaffeic acid (PCA) and AuNPs. We chose GBP as a model of a periplasmic binding protein given our group's previous successful experience with this binding protein in the development of biosensors. The conformational change induced by binding glucose alters the microenvironment of the electrode's surface that manifests as a change in its electrochemical signal. The GBP-L-DOPA/AuNP/PCA/SPCE (Fig. 1) demonstrated excellent selectivity toward glucose, both in phosphate buffer and human serum. The sensor had a dose-dependent response for glucose in the with a detection limit of 0.67 μM. The proposed sensor has the advantage to be reagentless as compared to enzyme-based sensors where there is a need to add substrates for generation of the product and/or signal. By incorporating unnatural electroactive amino acids to the protein that can be addressed by cyclic voltammetry, the sensor does not need any external addition of substrates to generate a signal that is dependent on the concentration of glucose in the sample. In addition, the developed sensor has a better detection limit than most of enzyme-based glucose sensors. This allows dilution of the sample before analysis which brings the concentration of potential interfering substances to below detection limits. Unlike enzyme biosensors that are typically reusable, the developed biosensor was designed to be a single use platform. To the best of our knowledge, this represents the first report of electrochemical detection of glucose via inherently electroactive amino acids incorporated into the primary sequence of a protein, thus broadening the application of unnatural amino acids in measurement science.

2. Material and methods

2.1. Reagents

Aqueous solutions were prepared using Milli-Q ultra-pure water with a resistance of 18.2 MΩ cm (MQ). Caffeic acid, 3,4-dihydroxyphenylalanine (L-DOPA) or 3-amino-L-tyrosine (NH_2Y), $HAuCl_4$, calcium chloride, magnesium sulfate, thiamine, ampicillin sodium salt, agarose, 2-[4-(2-hydroxyethyl) piperazin-1-yl] ethane sulfonic acid (HEPES), nitro blue tetrazolium (NBT), sodium glycine salt, sodium borate, D-glucose, fructose, sodium phosphate dibasic, sodium phosphate monobasic, acetic acid, all 20 amino acids, human serum, and glucose colorimetric/fluorometric assay kit were obtained from Sigma-Aldrich (St. Louis, MO). Ethyl alcohol 200 proof 99.5% was purchased from PHARMCO-AAPER (Brookfield, CT). The BCA protein assay kit and 3500 MWCO Slide-A-Lyzer 3 mL dialysis cassettes were from Thermo Fisher Scientific (Rockford, IL). ProBlock gold extra strength [100×] (protease inhibitor), Ni-NTA agarose resin, and isopropyl β-D-1-thiogalactopyranoside (IPTG) were obtained from Gold Biotechnology (St. Louis, MO). The Mark12 protein standard and 1 kb DNA standard were purchased from Invitrogen (Carlsbad, CA). All restriction digest enzymes, the plasmid pQE70, and QIAprep Spin Miniprep Kit were purchased from Qiagen (Redwood City, CA). Syringe filters (0.2 μm) were purchased from VWR (Bridgeport, NJ). Imidazole was obtained from J.T. Baker (Phillipsburg, NJ). Sodium dodecyl sulfate was ordered from Curtin Matheson (Houston, TX). Luria–Bertani (LB) broth was from Becton, Dickinson and Company (Sparks, MD). ATCC 23785 *E. coli* Phe auxotroph (Auxo) cells was from American Type Culture Collection (Manassas, VA).

2.2. Equipment

Screen-printed carbon electrodes ItalSens IS-C were purchased from PalmSens (Houten, Netherlands). Polymerase chain reactions (PCRs) were performed using an Eppendorf Mastercycler Personal Thermocycler (Hauppauge, NY). Electrophoresis of DNA was carried out using an FB105 Fisher Biotech Electrophoresis Power Supply (Pittsburgh, PA). DNA gels were visualized using a UV Transilluminator platform from

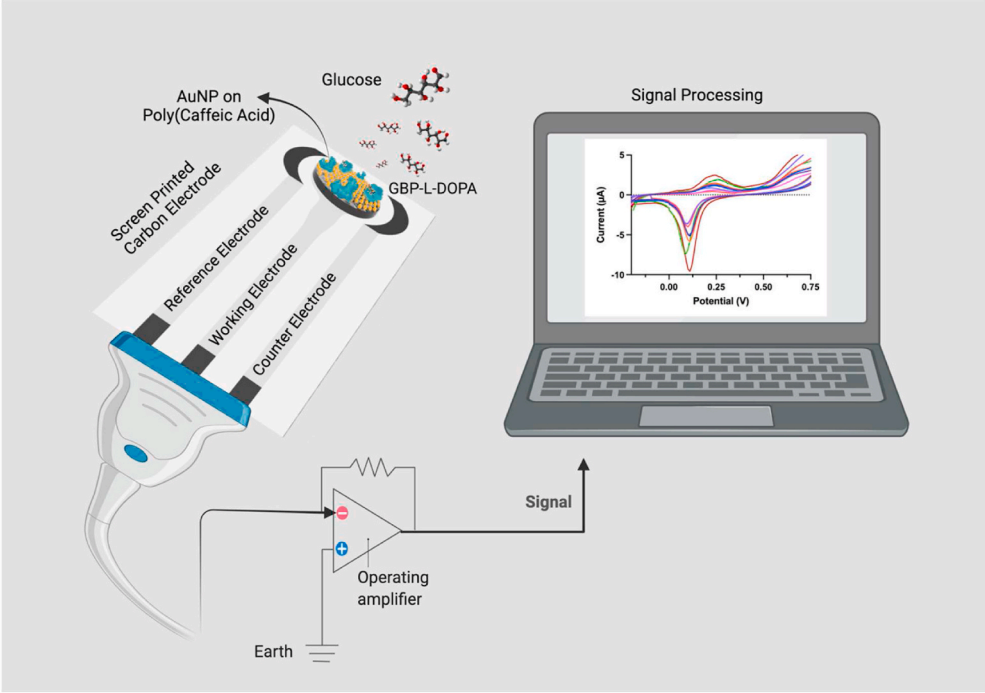

Fig. 1. Schematics of fabrication and analytical performance of the GBP-L-DOPA-based biosensor. Created with BioRender.com.

UVP (Upland, CA). The sonicator for lysing the cells was a 550 Sonic Dismembrator from Fisher Scientific. The incubator for the protein expression was a Forma Scientific Orbital Shaker (Fairlawn, NJ). All centrifugations were performed using a Beckman J2MI centrifuge (Palo Alto, CA). Proteins were visualized by sodium dodecyl sulfate polyacrylamide gel electrophoresis (SDS-PAGE) using PROTEAN TGX stain-free precast gels 4%–20% from Bio-Rad. Circular dichroism (CD) spectra were collected using a Jasco J-810 spectropolarimeter. Scanning electron microscopy (SEM) was used to study the morphology of the AuNPs using a Philips XL30 field-emission environmental SEM, operated at an acceleration voltage of 30 kV and a working distance of 10.1 mm. Amperometric and voltammetric measurements were performed with a PalmSens 4 electrochemical analyzer controlled by PSTrace5.3 software. A CLARIOstar Plus microplate reader (BMG LABTECH, Ortenberg, Germany) was used in the protein binding experiments.

2.3. DNA purification, isolation, and sequencing

For purification and isolation of plasmid DNA, a QIAprep Spin Miniprep Kit was used. The DNA was digested with restriction enzymes *Sph*I and *Hin*dIII. The resulting products were analyzed by TAE 1% agarose gel electrophoresis. DNA gels were visualized using a UV Transilluminator platform (Fig. S1). DNA sequencing was performed by GENEWIZ (South Plainfield, NJ) to confirm the correct DNA sequence.

2.4. Expression of proteins

GBP with a unique cysteine at position 152 was expressed with a 6x His tag at the C-terminus. The coding sequence for GBP was ligated into the *Sph*I – *Bam*HI sites of pQE70 (forward primer: TAAGCAGCATGCTTGATACTCGCATTGGTG and reverse primer TGCTTAAAGCTTAGTGATGGTGATGGTGAT). PCR was used to place a *Sph*I restriction site at the 5′ end and a *Bam*HI site at the 3’ end of the GBP coding sequence. The GBP gene contained a mutation to generate a unique cysteine at position 152 in place of histidine for labeling purposes (Table S1). Also, an alanine next to the N-terminal was changed to leucine. The plasmid was then transferred to *E. coli* Phe Auxo cell ATCC 23785. The *E coli* cells containing the recombinant DNA plasmid were grown on a plate containing LB and 200 mg mL^{-1} ampicillin. A single colony from the plate was collected. The cells were grown in 5 mL LB medium containing 200 mg mL^{-1} ampicillin overnight at 37 °C on an incubator/shaker. After centrifugation of the overnight culture, the cells were transferred into 300 mL fresh M9 medium containing 1x M9 salts, 0.4% (w/v) glucose, 1.0 mM $MgSO_4$, 0.1 mM $CaCl_2$, 100 mg each of 20 amino acids and 200 mg mL^{-1} ampicillin grown at 37 °C with shaking at 250 rpm to an OD_{600} of 0.6. The culture was then centrifuged at 5000×*g* for 15 min at 4 °C followed by resuspending and washing the pellet for three times with filter-sterilized 0.9% NaCl. The pellet was then resuspended in freshly prepared M9 media containing 1x M9 salts, 0.4% (w/v) glucose, 1.0 mM $MgSO_4$, 0.1 mM $CaCl_2$, 100 mg each of 19 amino acids excluding Phe. Cells were then grown for 1 h at 37 °C with shaking at 250 rpm. Protein expression was then induced with IPTG to 1 mM final concentration, 1.0 mM thiamin, and either 100 mg Phe or 600 mg L-DOPA, or 600 mg NH_2Y, or no amino acid or UAA to express GBP, GBP-L-DOPA, GBP-NH_2Y, and negative control (NC) respectively. The cultures were pelleted by centrifugation at 5000×*g* for 15 min, and the pellet was placed in lysis buffer (50 mM NaH_2PO_4, 30 mM NaCl, 10 mM imidazole, pH 8.0) followed by addition of protease inhibitor and lysed by sonication on ice, using a programmed cycle of 10 s on, 10 s off, for 20 min. The cell debris was pelleted by centrifugation at 17000×*g* for 20 min at 4 °C three times, and the resulting crude protein containing cell extract was removed to a separate culture tube. To the crude extract was added 1.0 mL of Ni-NTA resin, and this was mixed at room temperature for 1 h. The solution was then added to a gravity-flow column, and the flow-through was collected. The resin was washed with 20 mL of wash buffer (50 mM NaH_2PO_4, 30 mM NaCl, 20 mM imidazole, pH 8.0), and the wash fraction was collected. Purified protein was eluted from the column in 1.0 mL aliquots of elution buffer (50 mM NaH_2PO_4, 30 mM NaCl, 100 mM imidazole, pH 8.0). Proteins were visualized by SDS-PAGE (Fig. 2A), and the concentration of each aliquot was determined using the BCA assay kit. Purified proteins were dialyzed using 3500 MWCO Slide-A-Lyzer 3 mL dialysis cassettes in the final buffer against three changes of the buffer. The fractions containing purified proteins were filtered and stored at 4 °C. An aliquot of each sample was sent to Scripps Research Institute (Jupiter, FL) for liquid chromatography tandem mass spectrometry (LC-MS/MS) analysis (Fig. S2). The GBP and

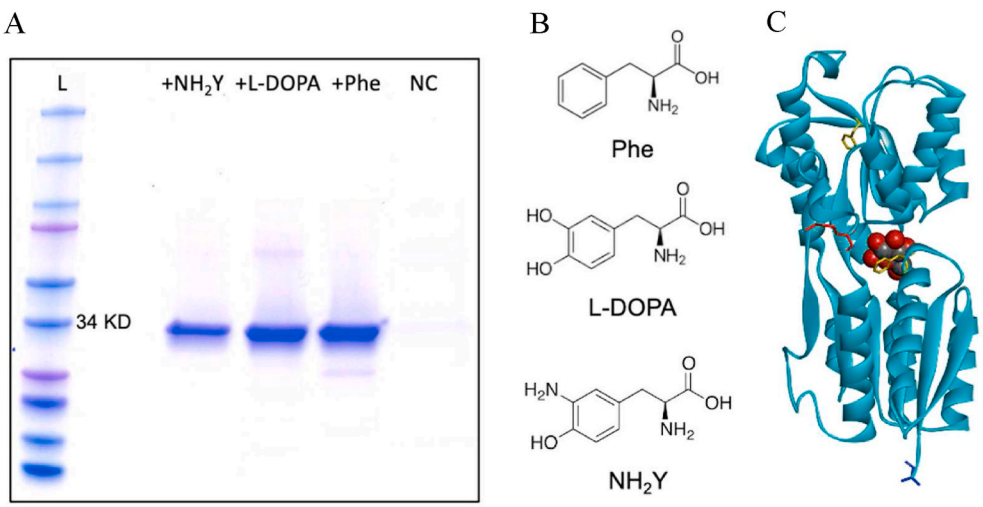

Fig. 2. A: Coomassie-stained SDS PAGE gel. Lanes: L, protein molecular weight marker; $+NH_2Y$, expressed with 19 amino acids and 3-amino-L-tyrosine; +L-DOPA, expressed with 19 amino acids and L-DOPA; +Phe, expressed with 19 amino acids and phenylalanine; NC, expressed with only 19 amino acids as a negative control. B: Chemical structure of phenylalanine, L-DOPA, and 3-amino-L-tyrosine. C: X-ray crystal structure of GBP with the bound β-D-glucose shown as a ball and stick figure. The X-ray crystal structure of the protein was visualized using Studio Visualizer (BIOVIA) by using the coordinates downloaded from the RCSB protein data bank (PDBID- 2GBP). The yellow Phe residues indicate sites of incorporation of L-DOPA in the GBP-L-DOPA.

GBP-L-DOPA demonstrated peaks at 34716 Da and 34747-34748 Da, (Fig. S2), respectively. LC-MS/MS of the protein gel-band digests found one Phe changed by mass shift of +31Da in the GBP-NH_2Y sample and two Phe changed by mass shift of +32Da in GBP-L-DOPA sample compared to native GBP. The LC-MS/MS was controlled by Thermo Scientifi Xcalibur software, and the data were analyzed by Scaffold Proteome Software. These peptides were found based on peptide spectral matches (PSMs).

2.5. NBT dot blotting

For the nitroblue tetrazolium (NBT) dot blotting assay, purified GBP and GBP-L-DOPA were prepared to a final concentration of 0.5 mg mL^{-1} in 10 mM acetic acid. Then, 2 μL of each GBP solution was dropped onto a nitrocellulose transfer membrane. The membrane was then immersed in 2.0 M sodium glycinate buffer (pH 10.0) containing 0.5 mg mL^{-1} NBT and incubated until a blue-purple color developed at room temperature. The stained membrane was washed with 0.2 M sodium borate solution (pH 8.5) and MQ water (Fig. S3).

2.6. Characterization of native and engineered GBPs

The purified GBPs were prepared in 10 mM HEPES buffer containing 0.2 mM $CaCl_2$ at pH 8.0. The GBPs were chemically modified via site-selective fluorescent labeling of the unique Cys residue with 10-fold molar excess of 7-diethylamino-3-((((2-maleimidyl)ethyl)amino) carbonyl) coumarin (MDCC) dissolved in DMSO, using the manufacturer's instructions. The labeling reaction was carried out overnight at 4 °C in an amber glass vial, protected from light. Following the labeling reaction, the protein was extensively dialyzed in 3500 MWCO dialysis cassettes in 10 mM HEPES buffer containing 0.2 mM $CaCl_2$ at pH 8.0 buffer to remove any excess MDCC and adjusted to a final concentration of 1×10^{-7} M. The proteins were characterized in terms of their binding ability using $10^{-8} - 10^{-1}$ M glucose. For the assay, 180 μL of the labeled protein solution was added to 20 μL of each glucose standard solution, as well as a blank, in triplicate in a clear microtiter plate; the contents were mixed gently and thoroughly, and the fluorescence was measured. MDCC was excited at a wavelength of 419 nm, and fluorescence emission was monitored at an emission wavelength of 466 nm with a CLARIOstar Plus Microplate reader. Upon glucose binding, the fluorescence intensity generated by the MDCC-labeled GBPs decreased. Since the MDCC-modified cysteine is located on a flexible region at the edge of the binding pocket, MDCC can experience a different environment as the protein changes conformation as a result of glucose binding (Fig. S4).

2.7. Determining the secondary structure of the protein using circular dichroism (CD)

Purified protein was dialyzed by 3500 MWCO Slide-A-Lyzer 3 mL dialysis cassettes in the buffer containing 10 mM phosphate, 0.2 mM $CaCl_2$, pH 7.4, against three changes of the buffer. Protein sample of GBP was determined to have a concentration of 100 μg mL^{-1}. Spectra were collected using a CD spectrophotometer (Fig. 3 and S5).

2.8. Fabrication and characterization of GBPs/AuNP/PCA/SPCE

The commercially available SPCEs (with screen printed carbon as the working electrode (W.E.), Ag/AgCl as the reference electrode, and Pt as the counter electrode) were pretreated by sweeping the potential from −1.0 to +1.0 V at a scan rate of 300 mV s^{-1} using cyclic voltammetry in 0.5 M sulfuric acid. Caffeic acid solutions were prepared freshly before polymerization and all experiments were carried out at room temperature. A thin layer of PCA was generated on the surface of SPCE by addition of 50 μL of 1.0 mM caffeic acid dissolved in 0.05 mM phosphate buffer (PB) solution, pH 6.0, by applying a chronoamperometric pulse at 2.0 V for 2 min. The surface of the electrodes was then rinsed with the PB solution. A volume of 30 μL of 1 mM gold(III) chloride ($HAuCl_4$) in PB solution, pH 7.4, placed on the surface of PCA/SPCE. The AuNP deposition was carried out by applying a potential of −0.6 V for 5 min to generate AuNP/PCA/SPCE. Cyclic voltammograms of the electrodes were collected by sweeping the potential from −0.2 to +1.0 V at a scan rate of 50–300 mV s^{-1} in 50 mM PB solution (Fig. S6). The presence of a significant reduction peak in the generated cyclic voltammograms indicated the successful AuNP deposition on electrodes. The morphology of the nanoparticles was examined using SEM. The size of 100 AuNPs was measured at the longest line of each particle on the micrographs, and the mean and standard deviation are reported to be 51 ± 12 nm. The surface of the electrodes was rinsed with PB, and then 10 μL of 250 μg mL^{-1} GBP, or GBP-L-DOPA, or GBP-NH_2Y were drop-casted on the surface of the distinct AuNP/PCA/SPCE electrodes to generate GBP/AuNP/PCA/SPCE, GBP-L-DOPA/AuNP/PCA/SPCE, or GBP-NH_2Y/AuNP/PCA/SPCE; the electrodes were sealed and kept at 4 °C for a minimum incubation time of 3 h to allow the protein to bind to the AuNPs. As we have reported previously, the AuNP electrode response is pH-dependent, and by decreasing the pH, the gold reduction peak shifts to higher potential (Zeynaloo et al., 2021a). After incubation, the surface of the electrodes was gently rinsed right before each use with PB solution, pH 7.4, to remove unbound proteins. For each detection step, 30 μL of each sample was placed on the surface of the electrode, and the response of each electrode was recorded by CV and differential pulse

voltammetry (DPV).

3. Results and discussion

Biosensors are molecular recognition devices consisting of biological and abiotic components that produce a signal upon ligand binding to the sensing element of the sensor in a manner that depends on the concentration of the ligand in the sample (Scheller et al., 2001). The biological components of biosensors, such as proteins, deoxyribonucleic acid (DNA), cells, and aptamers, are molecules that specifically recognize the analyte ligand (Estrela et al., 2016; Mohapatra et al., 2020). Electrochemical biosensors are one of the most commonly successfully used classes of sensors and mainly use potentiometry (Zeynaloo et al., 2021b), amperometry (Emir et al., 2021; Khumngern et al., 2021), or voltammetry (Azimi et al., 2021; Taşaltın et al., 2021) as their detection principles. These electrochemical sensors are generally fast, compatible with various media, easy to miniaturize, cost-effective, and require small sample volumes, making them well-suited for clinical applications.

3.1. Protein characterization

Incorporation of UAAs within a protein structure can be accomplished by either using amber codon suppression and tRNA/synthetase pairs or auxotrophic strains that are unable to synthesize a particular amino acid (Niu and Guo, 2013; Joel et al., 2014; Lee et al., 2019), thus expanding the genetic code of the parent protein. The former is used for site-selective incorporation of UAA, while the latter can be used to incorporate UAAs at one or more positions within the protein structure. Using such methods, more than 200 UAAs have been incorporated into proteins to enhance their properties or generate new functions (Vargas-Rodriguez et al., 2018). 3,4-Dihydroxyphenylalanine (L-DOPA) and 3-amino-L-tyrosine (NH_2Y) are redox-active UAAs that are analogues of the phenylalanine and tyrosine cognate amino acids. L-DOPA contains a catechol moiety that participates in a quasi-reversible, 2-electron redox process. L-DOPA and NH_2Y have been successfully incorporated into proteins to enhance their properties such as adhesion, water resistance, and polymerization or to apply in mechanistic studies as a redox active component (Ayyadurai et al., 2011; Yang et al., 2014b; Kim and Lee, 2018; Lee et al., 2018).

The incorporation of L-DOPA and NH_2Y in GBP was confirmed using SDS-PAGE, NBT dot blotting, and mass spectrometry. Specifically, the SDS-PAGE analysis clearly showed successful expression of GBP, GBP-L-DOPA, and GBP-NH_2Y (Fig. 2A). In the absence of Phe and UAAs no significant band of expressed protein was observed in the SDS-PAGE. This confirms that the auxotrophic *E. coli* requires Phe or analogues with similar structure such as L-DOPA (that includes two additional hydroxy groups) or NH_2Y (that contains one extra hydroxy and one extra amine group on its structure) to express the protein (Fig. 2B). Approximately 0.2–0.5 mg L^{-1} of purified engineered GBPs were obtained from a 250-mL scale culture after Ni-NTA affinity chromatographic purification.

The redox-dependent NBT dot blotting can be used to detect proteins containing L-DOPA (Yang et al., 2014a). An interesting property of L-DOPA is that it can reduce NBT causing a color change from the yellow tetrazolium salt to the formazan blue (Fig. S3). This allows screening for the incorporation of L-DOPA in proteins right from the culture. The results shown in Fig. S3 indicate the successful incorporation of L-DOPA in GBP. Through LC-MS/MS analysis, we additionally confirmed a mass difference indicative of L-DOPA and NH_2Y being incorporated in GBP-L-DOPA and GBP-NH_2Y, respectively. The incorporation of two L-DOPA molecules at the locations of Phe17 and Phe144 (Fig. 2C) and one NH_2Y at the location of Phe17 was demonstrated by LC-MS/MS.

Incorporation of UAAs analogues of cognate amino acids into a protein structure may result in changes in the microenvironment surrounding the amino acid, and potentially impact the overall protein properties, function, and stability. While such an impact should, in general, be less drastic than incorporating an extraneous label/reporter or generically fusing the protein to a reporter protein, the new protein still needs to be characterized in full to assess any loss of function or alteration of the properties when compared the parent protein. As mentioned before, we have previously developed a series of fluorescent biosensors using GBP extraneously labeled as well as with incorporated unnatural amino acids. In order to evaluate the ability of our newly electroactive GBP proteins to bind glucose and have a reference as a means of comparison with our prior biosensors, we followed methods employed earlier by us to covalently attach the fluorescent label MDCC to the cysteine residue at location 152 in the electroactive proteins. The response of the labeled GBPs was measured in standard glucose solutions by monitoring the changes in fluorescence intensity of MDCC. The fluorescence quenching of the native and engineered GBPs labeled with MDCC in solutions containing 10^{-8} – 10^{-1} M glucose was plotted, and the results are shown in Fig. S4. The native GBP K_D was estimated to be 1.4×10^{-6} M which is comparable to the reported binding constant of GBP (Joel et al., 2014). The K_D of GBP-L-DOPA and GBP-NH_2Y (1.1×10^{-5} M and 7.1×10^{-6} M, respectively) were slightly higher than that of the native GBP. The native GBP contains seven Phe residues in its structure, and Phe17 was replaced by NH_2Y in the GBP-NH_2Y, and two Phe (Phe17 and Phe144) were replaced by L-DOPA in GBP-L-DOPA. In both engineered GBPs, one of the Phe in the binding pocket was replaced with UAAs, which may explain the change in apparent K_D compared to native GBP.

To further study the structural modifications resulting from UAA incorporation, the thermal stability of the expressed GBPs was evaluated by CD spectroscopy (Fig. 3). Both GBP-L-DOPA and GBP-NH_2Y demonstrated similar CD spectra as native GBP, suggesting the absence of significant changes in the overall secondary structure of the proteins (Fig. 3A). All three GBPs consisted mostly of α-helical structures (peaks at approximately 210 and 220 nm). In development of protein-based biosensors, the protein thermal stability is an essential consideration in determining the lifetime of the biosensor. The melting temperature (T_m) of the GBP, GBP-L-DOPA, and GBP-NH_2Y were determined at 222 nm to be 46.7 ± 0.3 °C, 45.2 ± 0.5 °C, and 44.8 ± 0.5 °C, respectively (Fig. 3B). The similarity of the T_m among the three proteins is consistent with the similarity of the engineered GBPs' structures to the native GBP. The forward and reverse T_m measurements were also carried out (Fig. S5) to confirm the stability of the engineered proteins and their ability to fold back to their secondary structure after thermal denaturation. All three proteins demonstrated high stability and reversibility after thermal denaturation.

3.2. Electrode fabrication and characterization

Different nanomaterials and polymers have been combined to design nano-assembly systems with enriched electronic and electrocatalytic activities (Cai et al., 2007; Maity et al., 2019). Several electrochemical sensors have been reported using redox polymers, including polyphenols, as sensor modifiers (Setti et al., 2005; Liu et al., 2012; Xu et al., 2012; Li et al., 2016; Selvolini et al., 2019). Polycaffeic acid (PCA), a type of polyphenol, exhibits excellent electrochemical activity on different electrodes (gold, platinum, carbon, etc.) and has been used for electrode surface modification (Ren et al., 2006; Stasyuk et al., 2012; Li et al., 2016; Rohanifar et al., 2016; Zhang et al. 2019a, 2019b). PCA participates in reversible electron transfer and acts as a mediator in the reduction of the target molecule. Electropolymerization of caffeic acid to deposit a thin layer of PCA on the electrode surface can be carried out under potentiostatic conditions. The advantage of using constant potential (potentiostatic method) is that it can effectively reduce the probability of side reactions and, thus, generate polymers with stable structure, high electroactivity, and high purity.

The response of the SPCE electrodes was collected by sweeping the potential from −0.2 to 1.0 V after addition of each layer on the working electrode (Fig. 4A). The cyclic voltammogram of bare SPCE in PB

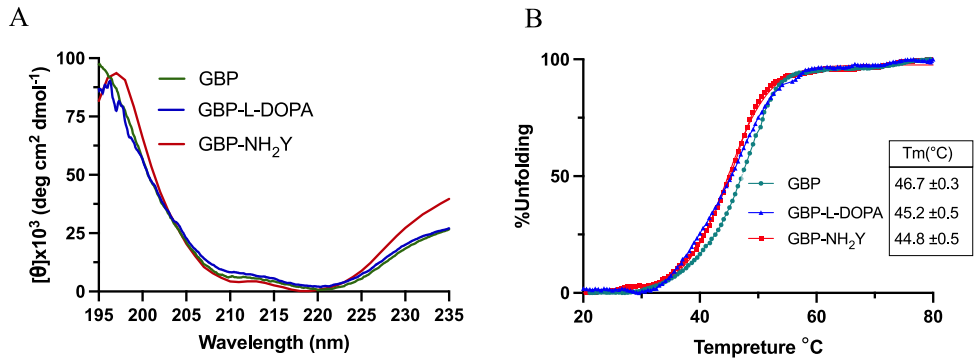

Fig. 3. A:CD absorbance of GBP, GBP-L-DOPA, and GBP-NH_2Y. Three accumulations were averaged for each sample at 20 °C. The response for each blank was subtracted from the response for the corresponding sample, and the resulting spectra are shown. B: Thermal denaturation curves for GBP, GBP-L-DOPA, and GBP-NH_2Y. Alpha helix denaturation was monitored by CD at 222 nm as the temperature was increased from 20 to 80 °C. inset: T_m values for GBP, GBP-L-DOPA, and GBP-NH_2Y. All T_m values are the average of three measurements. For the CD spectroscopy experiments, the proteins were prepared at a concentration of 100 μg mL^{-1} in 10 mM sodium phosphate buffer saline at pH 7.4.

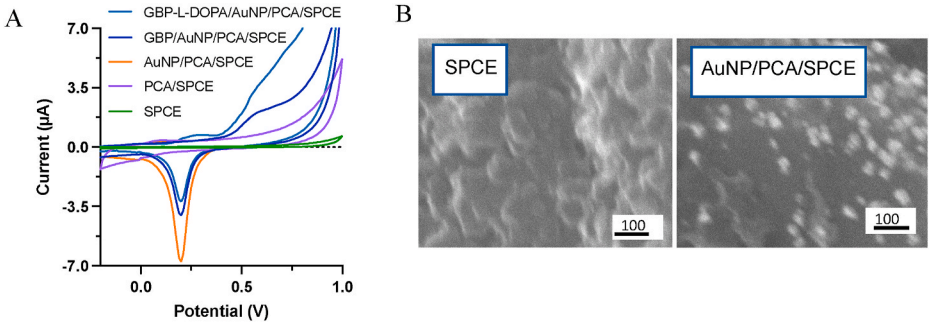

Fig. 4. A: Cyclic voltammograms of the modified SPCE electrode. Scanning range is from −0.2 V to +1.0 V vs. Ag/AgCl at a rate of 150 mV s^{-1} in 50 mM phosphate buffer at pH 7.4. B: Surface characterization of polycaffeic acid/AuNP-modified SPCEs using scanning electron microscopy (SEM).

solution at pH 7.4 was redox-inert. After polymerization of caffeic acid, the cyclic voltammograms of the PCA/SPCE were collected using several scan rates, and the plots of the anodic and cathodic peak currents vs. scan rate were linear (Fig. S6). These data confirm the reversible electron transfer of the quinone/hydroquinone portion of the polymerized caffeic acid on the surface of the SPCE. Then, AuNPs were deposited on the PCA/SPCE by electrochemical reduction of Au^{3+} to Au^0 on the surface of the polymerized working electrode to generate AuNP/PCA/SPCE electrodes. The generation of AuNPs on the surface of the electrodes was confirmed by the appearance of oxidation and reduction peaks at +0.59 V and +0.19 V, respectively.

Following immobilization of GBP-L-DOPA on either AuNP/SPCE or AuNP/PCA/SPCE, the cyclic voltammogram demonstrated an oxidation peak corresponding to L-DOPA at +0.24 V, which was enhanced significantly by addition of the polycaffeic acid film on the surface of the fabricated biosensor. However, there was no reproducible/significant peak observed from GBP-NH_2Y/AuNP/PCA/SPCE. Consequently, all subsequent studies reported herein were performed using GBP-L-DOPA/AuNP/PCA/SPCE as the fabricated biosensor. To confirm that the peak at +0.24 V is a result of the incorporated L-DOPA in the GBP and not the other protein residues, native GBP was immobilized on the electrode's surface; the CVs in Fig. 4A demonstrated the absence of a peak at +0.24 V.

To characterize the morphology of the electrochemically derived polymer nanocomposite, SEM analysis was performed with the SPCE and AuNP/PCA/SPCE electrodes (Fig. 4B). The deposited AuNPs have an average size of 51 ± 12 nm. In comparison to a prior study involving the direct deposition of AuNP on SPCE under similar conditions of gold concentration and potential (Zeynaloo et al., 2021a), the addition of a layer of PCA resulted in smaller and more uniform AuNP. A possible explanation is that, even though caffeic acid is an efficient mediator, it is less conductive in comparison with graphite (the bare SPCE), leading to slower deposition and less aggregation of the deposited AuNPs generated on PCA/SPCE.

3.3. Electrochemical impedance spectroscopy (EIS)

The surface polymerization of SPCE, AuNP generation, and protein conjugation on the surface of AuNP/PCA/SPCE were confirmed with electrochemical impedance spectroscopy (EIS). Fig. 5 shows the Nyquist plots for the bare SPCE, PCA/SPCE, AuNP/PCA/SPCE, and GBP-L-DOPA/AuNP/PCA/SPCE, which were obtained in 0.1 M KCl and 5 mM $K_3[Fe(CN)_6]$, 50 mM PBS at pH 7.4, in the frequency range of 100 mHz–100 MHz at a potential of +0.16 V (vs. Ag/AgCl) with an AC amplitude of 10 mV. The largest semicircle was observed with PCA/

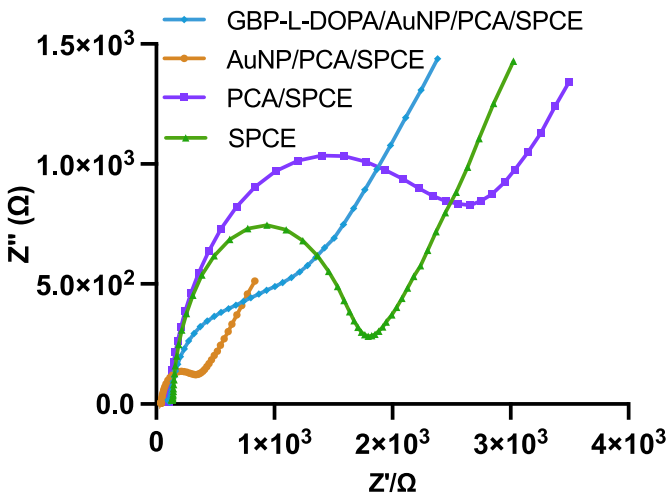

Fig. 5. Nyquist plots of the biosensors in 0.1 M KCl and 5 mM $K_3[Fe(CN)_6]$.

SPCE and was attributed to the lower conductivity of the thin film of polycaffeic acid on the surface of screen-printed carbon electrode. After addition of the AuNPs on the PCA/SPCE's surface, the W.E. conductivity increased significantly as demonstrated by the smallest semicircle (Fig. 5). However, after the GBP-L-DOPA conjugation on the electrode's surface, an increase in the diameter of the semicircle of the Nyquist plot was observed. This is attributed to the electron transfer resistance due to the conjugation of the less conductive protein molecule on the surface of the AuNP/PCA/SPCE.

3.4. Analytical performance of the fabricated electrochemical biosensor

The binding of GBP, GBP-L-DOPA, and GBP-NH_2Y to sense glucose in solution was confirmed through chemically labeling with a fluorescent marker (Fig. S4) (vide supra). Among fabricated electrochemical biosensors, the GBP-L-DOPA-based sensor demonstrated reproducible voltammograms. The cyclic voltammograms of the fabricated biosensor were obtained in the potential range of −0.2 to +1.0 V vs. Ag/AgCl in PB, pH 7.4, at a scan rate of 150 mV s^{-1}, and the peak current (i_{pa}) of the L-DOPA oxidation peak was recorded at +0.24 V. The peak current in the anodic scan decreased as the concentration of glucose increased (Fig. 6A **inset**, Fig. S7). The calibration plot of the difference in the i_{pa} at +0.24 V before and after addition of glucose versus glucose concentration was plotted. The data were fitted to a nonlinear model, and the best fit equation is shown in Fig. 6. The sensitivity of the sensor, as determined in the linear portion of the calibration plot in Fig. 6, is 0.30 A M^{-1}. A detection limit of 0.67 μM was calculated as the concentration corresponding to three standard deviations above the lowest Δi_{pa} (relevant to the lowest measured concentration signal). All measurements were performed in triplicate with three distinct biosensors. The reduction in the i_{pa} might be attributed to the conformational change of the GBP-L-DOPA after binding to glucose, which changes the overall protein conformation from the open to the closed form, subsequently altering the accessibility of L-DOPA when glucose is present. This is manifested as a change in the i_{pa} of the voltammograms. Electrons are transferred from the L-DOPA to the electrode surface by the PCA redox media, enabling the direct detection of glucose.

Differential pulse voltammetry (DPV) was also used to investigate the response of the GBP-L-DOPA/AuNP/PCA/SPCE electrode toward an increasing concentration of glucose (0.5–10 μM) in PB solution at a scan rate of 150 mV s^{-1}; the results are shown in Fig. 6B and Fig. S8. As it can be seen in the figure, the current decreased with increasing glucose concentration. The biosensor demonstrated stable responses over the entire concentration range with a rapid response time of less than 60 s.

To investigate the specificity of the GBP-L-DOPA/AuNP/PCA/SPCE biosensor toward glucose, the effect of other sugars such as fructose, maltose, sucrose, and two commonly encountered interferents in biological samples, ascorbic acid (AA) and uric acid (UA), was determined in PB solution at pH 7.4. The selectivity of the biosensor was measured in the presence of 1.0–15.0 μM of each potentially interfering compound. The signal from the three sugars was low, consistent with the selectivity of GBP toward binding glucose (Fig. 6C). At 1.0 μM of AA and UA there was no significant interference observed. Human serum at fasting contains 3.9–7.2 mM glucose (Danaei et al., 2011), while the concentrations of UA and AA are 208–417 μM (Feig et al., 2006; Karlsen et al., 2007) and 34–114 μM, respectively. Because of the ability of the sensor to

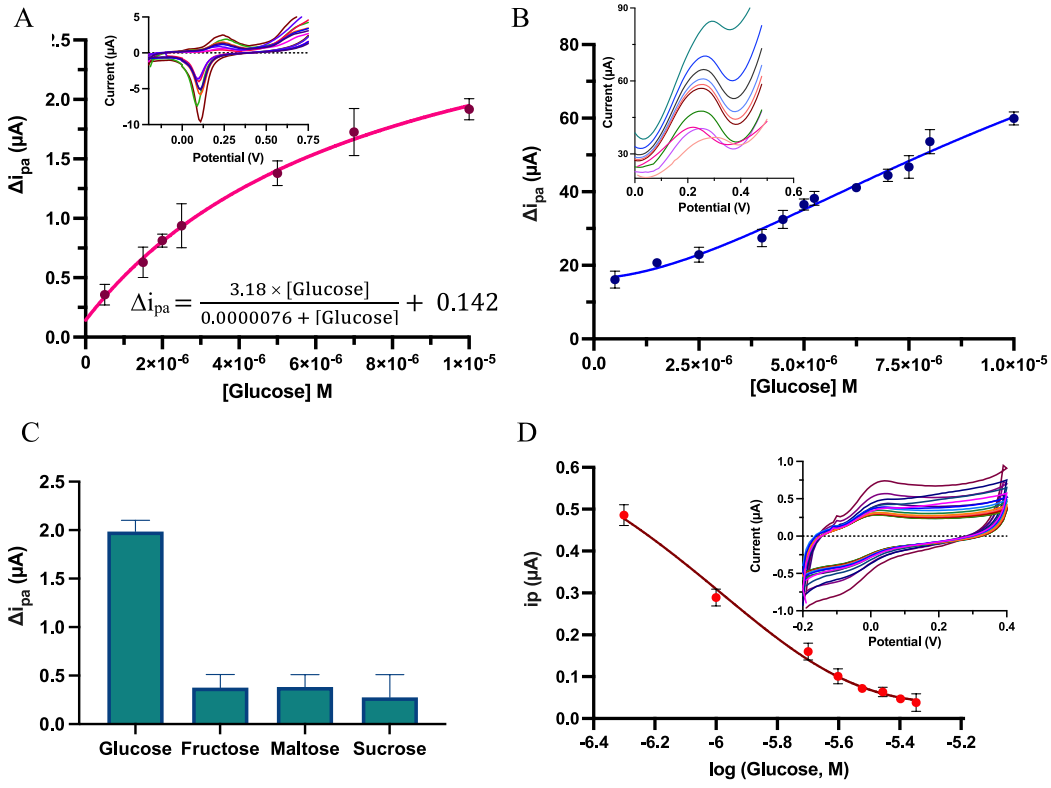

Fig. 6. A. Calibration plot for the change in the L-DOPA oxidation peak current (measured at +0.24 V) vs glucose concentration from CV scans. Inset: Cyclic voltammograms of GBP-L-DOPA/AuNP/PCA/SPCE in 50 mM PB, pH 7.4 in the presence of different glucose concentrations. The region of the oxidation peak expanded for easier visualization in Fig. S7. The best fit nonlinear response equation is also shown. **B.** Calibration plot for the change in the L-DOPA oxidation peak current vs glucose concentration from DPV scans. Inset: Differential pulse voltammograms of GBP-L-DOPA/AuNP/PCA/SPCE in 50 mM PB, pH 7.4 in the presence of different glucose concentrations. The L-DOPA oxidation peaks were expanded and labeled for easier visualization in Fig. S8.**C.** Cross-reactivity of the biosensor with fructose, maltose, and sucrose at concentration of 15 μM. The data represent the percent change of current at +0.24 V in triplicate. Data are baseline-subtracted using GBP-L-DOPA/AuNP/PCA/SPCE.**D.** Spiking of diluted human serum (1:1000) with 0.5 μM–4.5 μM glucose (to final concentration of 4.7–8.7 μM). Inset: Cyclic voltammograms of GBP-L-DOPA/AuNP/PCA/SPCE in 1:1000 diluted human serum with 50 mM PB, pH 7.4, in the presence of different glucose concentrations.

detect micromolar range of glucose levels, the human serum sample can be diluted 1000-fold prior to analysis. This has the added benefit of diluting both UA and AA level to concentrations that do not pose interference with the biosensor. To demonstrate the ability of the biosensor to detect glucose in human serum, standards were prepared with known concentrations of glucose in diluted human serum and the CV of the fabricated biosensor was obtained by sweeping the potential from −0.2 to +0.4 V at a scan rate of 150 mV s^{-1}. To accomplish this, the level of glucose in stock human serum was first evaluated with a glucose colorimetric kit to be 4.1 mM. The human serum was then spiked by adding glucose in the concentration range of 0.5–4.5 μM (corresponding to 4.6–8.6 mM glucose levels in undiluted serum). The results showed that the fabricated biosensor had a dose-dependent response toward glucose in the biological sample without any redox peak arising from interferences (Fig. 6D). To further evaluate the biosensor, samples were prepared with a known concentration of glucose (5.6 μM) and evaluated in triplicate using the calibration plot of Fig. 6D. The recovery percentages were calculated to be 92.23% ± 0.06 at 5.6 μM.

4. Conclusion

In conclusion, this study demonstrates the development of a new biosensor platform for analyte detection by incorporating an UAA within a model protein, namely GBP, that functions as an electroactive bioreporter. The electroactive GBP was immobilized onto gold nanoparticle-modified, polymerized caffeic acid, screen-printed carbon electrodes (GBP-L-DOPA/AuNP/PCA/SPCE). The UAA incorporated GBPs was able to act as a label/reporter to selectively and directly detect glucose electrochemically by CV and DPV. The developed reagentless biosensor was highly selective and sensitive towards glucose with a detection limit of 0.67 μM in buffer and a percent recovery of 92.23% ± 0.06 in human serum. The current study serves as a proof-of-concept of the global incorporation of an electroactive amino acid into the protein's primary sequence that can be used as a label for the highly selective electrochemical detection of analytes of interest.

Declaration of competing interest

The authors declare that they have no known competing financial interests or personal relationships that could have appeared to influence the work reported in this paper.

Acknowledgements

EZ and LGB thank University of Miami Department of Chemistry.

SD thanks the following grants from the NIH R01GM127706 and 1R01MH110415- 01A1; NSF-CBET-1841419 and CBET-2041413; and Firefighters Cancer Initiative State of Florida appropriation #2382A.

SD is also grateful to the NIH for grants R01MH104656 and UL1TR002736, and to the Miller School of Medicine of the University of Miami for the Lucille P. Markey Chair of Biochemistry and Molecular Biology. Fig. 1 was created with BioRender.com.

Appendix A. Supplementary data

Supplementary data to this article can be found online at https://doi.org/10.1016/j.bios.2021.113861.

References

Ayyadurai, N., Prabhu, N.S., Deepankumar, K., Jang, Y.J., Chitrapriya, N., Song, E., Lee, N., Kim, S.K., Kim, B.G., Soundrarajan, N., Lee, S., Cha, H.J., Budisa, N., Yun, H., 2011. Bioconjugation of L-3,4-dihydroxyphenylalanine containing protein with a polysaccharide. Bioconjugate Chem. 22 (4), 551–555.

Azimi, S., Farahani, A., Docoslis, A., Vahdatifar, S., 2021. Developing an integrated microfluidic and miniaturized electrochemical biosensor for point of care determination of glucose in human plasma samples. Anal. Bioanal. Chem. 413 (5), 1441–1452.

Bachas, L., Zeynaloo, E., Yang, Y., Manfredi, A., Careri, M., Deo, S., Daunert, S., 2019. Design of a mediator-free non-enzymatic electrochemical biosensor for glutamate detection. J. Cerebr. Blood Flow Metabol. SAGE PUBLICATIONS INC 2455 TELLER RD, THOUSAND OAKS, CA 91320 USA.

Bagdziunas, G., Palinauskas, D., 2020. Poly(9h-Carbazole) as a organic semiconductor for enzymatic and non-enzymatic glucose sensors. Biosensors 10 (9).

Cai, D., Yu, Y., Lan, Y., Dufort, F.J., Xiong, G., Paudel, T., Ren, Z., Wagner, D.J., Chiles, T. C., 2007. Glucose sensors made of novel carbon nanotube-gold nanoparticle composites. Biofactors 30 (4), 271–277.

Danaei, G., Finucane, M.M., Lu, Y., Singh, G.M., Cowan, M.J., Paciorek, C.J., Lin, J.K., Farzadfar, F., Khang, Y.H., Stevens, G.A., Rao, M., Ali, M.K., Riley, L.M., Robinson, C. A., Ezzati, M., Global, G., Burden of Metabolic Risk Factors of Chronic Diseases Collaborating, 2011. National, regional, and global trends in fasting plasma glucose and diabetes prevalence since 1980: systematic analysis of health examination surveys and epidemiological studies with 370 country-years and 2.7 million participants. Lancet 378 (9785), 31–40.

Ehrick, J.D., Luckett, M.R., Khatwani, S., Wei, Y., Deo, S.K., Bachas, L.G., Daunert, S., 2009. Glucose responsive hydrogel networks based on protein recognition. Macromol. Biosci. 9 (9), 864–868.

Emir, G., Dilgin, Y., Ramanaviciene, A., Ramanavicius, A., 2021. Amperometric nonenzymatic glucose biosensor based on graphite rod electrode modified by Ni-Nanoparticle/Polypyrrole composite. Microchem. J. 161.

Estrela, P., Bhalla, N., Jolly, P., Formisano, N., Estrela, P., 2016. Introduction to biosensors. Essays Biochem. 60 (1), 1–8.

Fazio, E., Spadaro, S., Corsaro, C., Neri, G., Leonardi, S.G., Neri, F., Lavanya, N., Sekar, C., Donato, N., Neri, G., 2021. Metal-oxide based nanomaterials: synthesis, characterization and their applications in electrical and electrochemical sensors. Sensors 21 (7).

Feig, D.I., Mazzali, M., Kang, D.H., Nakagawa, T., Price, K., Kannelis, J., Johnson, R.J., 2006. Serum uric acid: a risk factor and a target for treatment? J. Am. Soc. Nephrol. 17 (4 Suppl. 2), S69–S73.

Heo, N.S., Zheng, S., Yang, M., Lee, S.J., Lee, S.Y., Kim, H.-J., Park, J.Y., Lee, C.-S., Park, T.J., 2012. Label-free electrochemical diagnosis of viral antigens with genetically engineered fusion protein. Sensors 12 (8), 10097–10108.

Joel, S., Turner, K.B., Daunert, S., 2014. Glucose recognition proteins for glucose sensing at physiological concentrations and temperatures. ACS Chem. Biol. 9 (7), 1595–1602.

Karlsen, A., Blomhoff, R., Gundersen, T.E., 2007. Stability of whole blood and plasma ascorbic acid. Eur. J. Clin. Nutr. 61 (10), 1233–1236.

Kato, Y., 2015. An engineered bacterium auxotrophic for an unnatural amino acid: a novel biological containment system. PeerJ 3.

Khumngern, S., Jirakunakorn, R., Thavarungkul, P., Kanatharana, P., Numnuam, A., 2021. A highly sensitive flow injection amperometric glucose biosensor using a gold nanoparticles/polytyramine/prussian blue modified screen-printed carbon electrode. Bioelectrochemistry 138.

Kim, S., Lee, H.S., 2018. Genetic incorporation of biosynthesized L-dihydroxyphenylalanine (dopa) and its application to protein conjugation. JoVE 138.

Lee, K.J., Kang, D., Park, H.S., 2019. Site-specific labeling of proteins using unnatural amino acids. Mol. Cell. 42 (5), 386–396.

Lee, W., Kasanmascheff, M., Huynh, M., Quartararo, A., Costentin, C., Bejenke, I., Nocera, D.G., Bennati, M., Tommos, C., Stubbe, J., 2018. Properties of site-specifically incorporated 3-aminotyrosine in proteins to study redox-active tyrosines: Escherichia coli ribonucleotide reductase as a paradigm. Biochemistry 57 (24), 3402–3415.

Li, T., Xu, J., Zhao, L., Shen, S., Yuan, M., Liu, W., Tu, Q., Yu, R., Wang, J., 2016. Au nanoparticles/poly(caffeic acid) composite modified glassy carbon electrode for voltammetric determination of acetaminophen. Talanta 159, 356–364.

Liu, S., Xing, X., Yu, J., Lian, W., Li, J., Cui, M., Huang, J., 2012. A novel label-free electrochemical aptasensor based on graphene-polyaniline composite film for dopamine determination. Biosens. Bioelectron. 36 (1), 186–191.

Looger, L.L., Dwyer, M.A., Smith, J.J., Hellinga, H.W., 2003. Computational design of receptor and sensor proteins with novel functions. Nature 423 (6936), 185–190.

Maity, D., R, M.C., T, R.K.R., 2019. Glucose oxidase immobilized amine terminated multiwall carbon nanotubes/reduced graphene oxide/polyaniline/gold nanoparticles modified screen-printed carbon electrode for highly sensitive amperometric glucose detection. Mater. Sci. Eng. C 105.

Mathew, M., Sandhyarani, N., 2014. Detection of glucose using immobilized bienzyme on cyclic bisureas-gold nanoparticle conjugate. Anal. Biochem. 459, 31–38.

Mohapatra, S.S., Frisina, R.D., Mohapatra, S., Sneed, K.B., Markoutsa, E., Wang, T., Dutta, R., Damnjanovic, R., Phan, M.-H., Denmark, D.J., Biswal, M.R., McGill, A.R., Green, R., Howell, M., Ghosh, P., Gonzalez, A., Ahmed, N.T., Borresen, B., Farmer, M., Gaeta, M., Sharma, K., Bouchard, C., Gamboni, D., Martin, J., Tolve, B., Singh, M., Judy, J.W., Li, C., Santra, S., Daunert, S., Zeynaloo, E., Gelfand, R.M., Lenhert, S., McLamore, E.S., Xiang, D., Morgan, V., Friedersdorf, L.E., Lal, R., Webster, T.J., Hoogerheide, D.P., Nguyen, T.D., D'Souza, M.J., Çulha, M., Kondiah, P.P.D., Martin, D.K., 2020. Advances in translational nanotechnology: challenges and opportunities. Appl. Sci. 10 (14).

Niu, W., Guo, J., 2013. Expanding the Chemistry of fluorescent protein biosensors through genetic incorporation of unnatural amino acids. Mol. Biosyst. 9 (12), 2961–2970.

Palani, K., Kumaran, D., Burley, S.K., Swaminathan, S., 2012. Structure of a periplasmic glucose-binding protein fromthermotoga maritima. Acta Crystallogr. F Struct. Biol. Crystal. Commun. 68 (12), 1460–1464.

Ren, W., Luo, H., Li, N., 2006. Electrochemical behavior of epinephrine at a glassy carbon electrode modified by electrodeposited films of caffeic acid. Sensors 6 (2), 80–89.
Rerngglit, W., Teanphonkrang, S., Suginta, W., Schulte, A., 2019. Amperometric enzymatic sensing of glucose using porous carbon nanotube films soaked with glucose oxidase. Mikrochim. Acta 186 (9), 616.
Rohanifar, A., Devasurendra, A.M., Young, J.A., Kirchhoff, J.R., 2016. Determination of L-dopa at an optimized poly(caffeic acid) modified glassy carbon electrode. Anal. Methods 8 (44), 7891–7897.
Salins, L.L., Ware, R.A., Ensor, C.M., Daunert, S., 2001a. A novel reagentless sensing system for measuring glucose based on the galactose/glucose-binding protein. Anal. Biochem. 294 (1), 19–26.
Salins, L.L.E., Ware, R.A., Ensor, C.M., Daunert, S., 2001b. A novel reagentless sensing system for measuring glucose based on the galactose/glucose-binding protein. Anal. Biochem. 294 (1), 19–26.
Scheller, F.W., Wollenberger, U., Warsinke, A., Lisdat, F., 2001. Research and development in biosensors. Curr. Opin. Biotechnol. 12 (1), 35–40.
Sehit, E., Drzazgowska, J., Buchenau, D., Yesildag, C., Lensen, M., Altintas, Z., 2020. Ultrasensitive nonenzymatic electrochemical glucose sensor based on gold nanoparticles and molecularly imprinted polymers. Biosens. Bioelectron. 165, 112432.
Selvolini, G., Lazzarini, C., Marrazza, G., 2019. Electrochemical nanocomposite single-use sensor for dopamine detection. Sensors 19 (14).
Setti, L., Fraleoni-Morgera, A., Ballarin, B., Filippini, A., Frascaro, D., Piana, C., 2005. An amperometric glucose biosensor prototype fabricated by thermal inkjet printing. Biosens. Bioelectron. 20 (10), 2019–2026.
Smolskaya, S., Andreev, Y., 2019. Site-specific incorporation of unnatural amino acids into Escherichia coli recombinant protein: methodology development and recent achievement. Biomolecules 9 (7).
Stasyuk, N., Smutok, O., Gayda, G., Vus, B., Koval'chuk, Y., Gonchar, M., 2012. Bi-enzyme L-arginine-selective amperometric biosensor based on ammonium-sensing polyaniline-modified electrode. Biosens. Bioelectron. 37 (1), 46–52.
Strømgaard, A., Jensen, A.A., Strømgaard, K., 2004. Site-specific incorporation of unnatural amino acids into proteins. Chembiochem 5 (7), 909–916.
Taşaltın, C., Türkmen, T.A., Taşaltın, N., Karakuş, S., 2021. Highly sensitive non-enzymatic electrochemical glucose biosensor based on pani: B12 borophene. J. Mater. Sci. Mater. Electron. 32 (8), 10750–10760.
Teasley Hamorsky, K., Ensor, C.M., Wei, Y., Daunert, S., 2008. A bioluminescent molecular switch for glucose. Angew. Chem. 120 (20), 3778–3781.
Teran-Alcocer, A., Bravo-Plascencia, F., Cevallos-Morillo, C., Palma-Cando, A., 2021. Electrochemical sensors based on conducting polymers for the aqueous detection of biologically relevant molecules. Nanomaterials 11 (1).
Vargas-Rodriguez, O., Sevostyanova, A., Soll, D., Crnkovic, A., 2018. Upgrading aminoacyl-trna synthetases for genetic code expansion. Curr. Opin. Chem. Biol. 46, 115–122.
Vyas, N.K., Vyas, M.N., Quiocho, F.A., 1988. Sugar and signal-transducer binding sites of the Escherichia coli galactose chemoreceptor protein. Science 242 (4883), 1290–1295.
Wang, L., Schultz, P.G., 2002. Expanding the genetic code. Chem. Commun. (1), 1–11.
Xu, F., Ru, H.-Y., Sun, L.-X., Zou, Y.-J., Jiao, C.-L., Wang, T.-Y., Zhang, J.-M., Zheng, Q., Zhou, H.-Y., 2012. A novel sensor based on electrochemical polymerization of diglycolic acid for determination of acetaminophen. Biosens. Bioelectron. 38 (1), 27–30.
Yang, B., Ayyadurai, N., Yun, H., Choi, Y.S., Hwang, B.H., Huang, J., Lu, Q., Zeng, H., Cha, H.J., 2014a. In vivo residue-specific dopa-incorporated engineered mussel bioglue with enhanced adhesion and water resistance. Angew. Chem. 126 (49), 13578–13582.
Yang, B., Ayyadurai, N., Yun, H., Choi, Y.S., Hwang, B.H., Huang, J., Lu, Q., Zeng, H., Cha, H.J., 2014b. In vivo residue-specific dopa-incorporated engineered mussel bioglue with enhanced adhesion and water resistance. Angew Chem. Int. Ed. Engl. 53 (49), 13360–13364.
Zeng, Y., Zhu, Z., Du, D., Lin, Y., 2016. Nanomaterial-based electrochemical biosensors for food safety. J. Electroanal. Chem. 781, 147–154.
Zeynaloo, E., Yang, Y.-P., Dikici, E., Landgraf, R., Bachas, L.G., Daunert, S., 2021a. Design of a mediator-free, non-enzymatic electrochemical biosensor for glutamate detection. Nanomed. Nanotechnol. Biol. Med. 31.
Zeynaloo, E., Zahran, E.M., Fatila, E.M., Flood, A.H., Bachas, L.G., 2021b. Anion-selective electrodes based on a ch-hydrogen bonding bis-macrocyclic ionophore with a clamshell architecture. Anal. Chem. 93 (13), 5412–5419.
Zhang, W., Zong, L., Liu, S., Pei, S., Zhang, Y., Ding, X., Jiang, B., Zhang, Y., 2019a. An electrochemical sensor based on electro-polymerization of caffeic acid and Zn/Ni-Zif-8-800 on glassy carbon electrode for the sensitive detection of acetaminophen. Biosens. Bioelectron. 131, 200–206.
Zhang, W., zong, L., Liu, S., pei, S., Zhang, Y., Ding, X., Jiang, B., Zhang, Y., 2019b. An electrochemical sensor based on electro-polymerization of caffeic acid and Zn/Ni-Zif-8–800 on glassy carbon electrode for the sensitive detection of acetaminophen. Biosens. Bioelectron. 131, 200–206.